

## Supporting Information

### Evidence for Polarity- and Viscosity-Controlled Pathways in the Termination Reaction in the Radical Polymerization of Acrylonitrile

Xiaopei Li,<sup>1</sup> Tasuku Ogihara,<sup>1</sup> Tatsuhisa Kato,<sup>1</sup> Yasuyuki Nakamura,<sup>2,\*</sup> and Shigeru Yamago<sup>1,\*</sup>

<sup>1</sup> Institute for Chemical Research, Kyoto University, Uji 611-0011, Japan

<sup>2</sup> Research and Services division of Materials Data and Integrated System, National Institute for Material Science, 1-2-1 Sengen, Tsukuba Ibaraki 305-0047, Japan

## Index

1. Termination reaction starting from **6**
  - 1-1. Termination reaction starting from **6b** and **6a** under different conditions
  - 1-2. Relation between *Disp/CC-Comb/CN-Comb* selectivity to temperature in Kelvin and bulk viscosity
  - 1-3. Relation between *Disp/CC-Comb/CN-Comb* selectivity to microviscosity
  - 1-4. Analyses of the effect of the polarity parameters of solvents to the *CN-Comb* selectivity
2. Thermal decomposition of **5**
3. NMR spectra
4. Cartesian coordinates
5. References

## 1. Termination reaction starting from 6

### 1-1. Termination reaction starting from **6b** and **6a** under different conditions

**Table S1.** The termination reactions of **1b** or **1a** starting from **6b** or **6a**, respectively.

Run	Precursor ( <b>6</b> )	Solvent	Temp. (°C)	Time (h)	Conv. (%)	Yield (%) <sup>a</sup>			
						<b>2</b>	<b>3</b>	<b>4</b>	<b>5</b>
1	<b>6b</b>	C <sub>6</sub> D <sub>6</sub>	60	2	99	3	4	45	44
2	<b>6b</b>	C <sub>6</sub> D <sub>6</sub>	50	2	99	3	5	44	43
3	<b>6b</b>	C <sub>6</sub> D <sub>6</sub>	40	2	99	4	5	43	43
4	<b>6b</b>	C <sub>6</sub> D <sub>6</sub>	25	3	99	5	6	42	44
5	<b>6b</b>	DMF	60	2	99	6	6	70	10
6	<b>6b</b>	DMF	86	2	90	9	10	55	11
7	<b>6b</b>	DMF	40	2	84	8	9	48	10
8	<b>6b</b>	DMF	25	2	80	10	10	47	9
9	<b>6b</b>	EC <sup>b</sup>	60	2	99	11	13	51	12
10	<b>6b</b>	EC <sup>b</sup>	50	2	86	12	13	44	10
11	<b>6b</b>	EC <sup>b</sup>	40	4	99	17	18	43	12
12	<b>6b</b>	PEG400	60	3	81	22	30	14	<1
13	<b>6b</b>	PEG400	50	4	84	11	34	13	<1
14	<b>6b</b>	PEG400	40	6	93	30	40	7	<1
15	<b>6b</b>	PEG400	25	10	63	25	28	2	<1
16	<b>6b</b>	Hexane	25	3	99	5	5	34	51
17	<b>6b</b>	CH <sub>2</sub> Cl <sub>2</sub>	25	3	99	5	7	50	32
18	<b>6b</b>	THF	25	3	89	8	10	47	29
19	<b>6b</b>	Acetone-d <sub>6</sub>	25	3	99	5	5	58	26
20	<b>6b</b>	CD <sub>3</sub> CN	25	2	99	4	5	65	20
21	<b>6a</b>	DMF	60	4	99	- <sup>c</sup>	9	- <sup>c</sup>	15
22	<b>6a</b>	DMF	50	5	99	- <sup>c</sup>	10	- <sup>c</sup>	15
23	<b>6a</b>	DMF	40	8	99	- <sup>c</sup>	12	- <sup>c</sup>	15
24	<b>6a</b>	DMF	25	10	99	- <sup>c</sup>	13	- <sup>c</sup>	15
25	<b>6a</b>	EC <sup>b</sup>	60	6	99	- <sup>c</sup>	16	- <sup>c</sup>	18
26	<b>6a</b>	EC <sup>b</sup>	50	8	99	- <sup>c</sup>	17	- <sup>c</sup>	18
27	<b>6a</b>	EC <sup>b</sup>	40	10	99	- <sup>c</sup>	20	- <sup>c</sup>	18

<sup>a</sup>Determined by <sup>1</sup>H NMR. <sup>b</sup>Ethylene carbonate. <sup>c</sup>The yields of **2b** and **4b** could be not determined by <sup>1</sup>H NMR due to the overlapping with solvent signals.

**1-2. Relation between Disp/CC-Comb/CN-Comb selectivity to temperature in Kelvin and bulk viscosity**

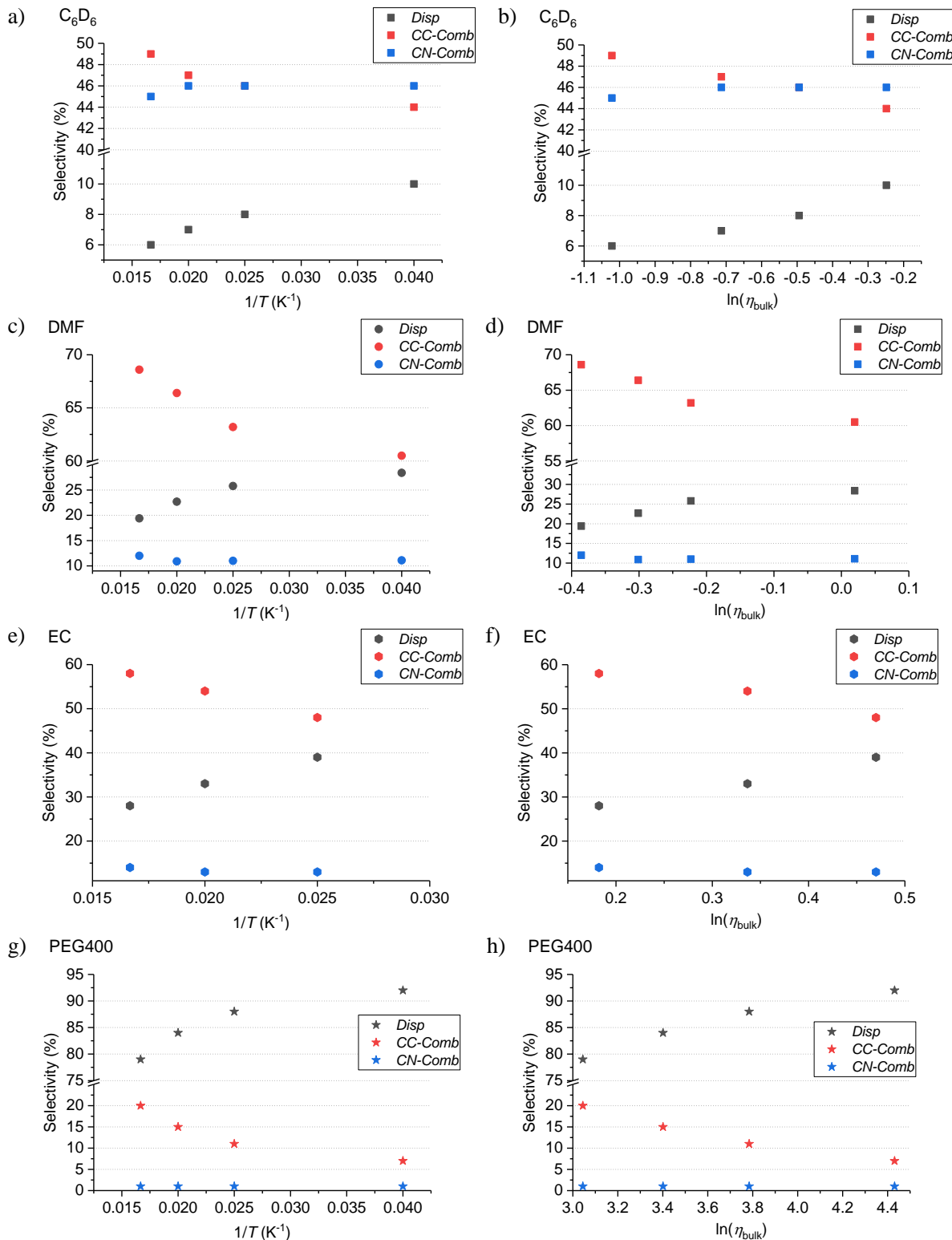


**Figure S1.** Correlation between the selectivity (Disp, CC-Comb, and CN-Comb) and temperature or bulk viscosity in termination reaction of **1b** in (a, b) C<sub>6</sub>D<sub>6</sub>, (c, d) DMF, (e, f) EC, (g, h) PEG400 at different temperature (see Table S1).

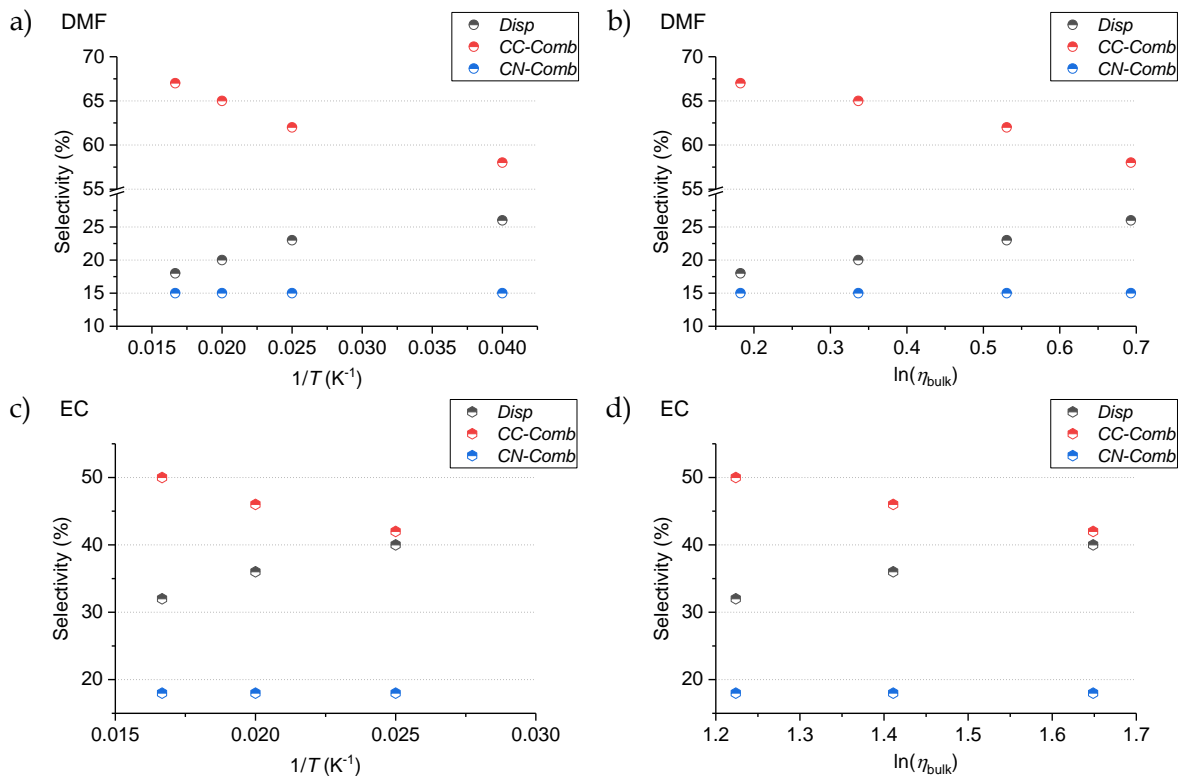


**Figure S2.** Correlation between the selectivity (*Disp*, *CC-Comb*, and *CN-Comb*) and temperature or bulk viscosity in the termination reaction of **1a** in (a, b) DMF, (c, d) EC at different temperature (see Table S1).

### 1-3. Relation between *Disp/CC-Comb/CN-Comb* selectivity to microviscosity

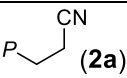
Microviscosity ( $\eta_{\text{micro}}$ ) was determined by Stokes-Einstein equation (1) with the obtained diffusion constant. The radius  $r$  of a molecule was estimated from the molecular volume obtained by theoretical calculations<sup>1</sup> for propionitrile and by hydrodynamic volume of **2a** measured by dynamic light scattering (DLS) assuming the spherical shape (Table S2).

$$D = \frac{k_B T}{6\pi\eta_{\text{micro}} r} \quad (1)$$

where  $k_B$  and  $T$  are is the Boltzmann coefficient ( $1.380 \times 10^{-23} \text{ kg m}^2 \text{ s}^{-2} \text{ K}^{-1}$ ) and absolute temperature in Kelvin.

The hydrodynamic diameter of **2a** ( $M_n = 2400$ ,  $D = 1.10$ ) was determined by DLS measurement using the backscattering angle of 165 ° for the solutions of **2a** in DMF (0.05 mol mL $^{-1}$ ) at 25 °C. The hydrodynamic diameter of **2a** was determined as 46 nm.

**Table S2.** Molecular volume and diffusion constant of radical and the model compounds.

Molecule	Molecular radius ( $\text{\AA}^3$ )	Solvent	Temp. (°C)	Diffusion constant ( $\times 10^{-9} \text{ m}^2 \text{ s}^{-1}$ )	$\eta_{\text{micro}}$ (mPa s)
 <b>(1b)</b>	86.4 <sup>a</sup>				
 <b>(2b)</b>	90.1 <sup>a</sup>	C <sub>6</sub> D <sub>6</sub>	120	11.4	0.070
			100	9.50	0.090
			80	6.36	0.12
			60	4.30	0.14
			50	3.63	0.15
			40	3.25	0.17
			25	2.76	0.21
			100	4.25	0.16
			80	3.56	0.18
			60	2.74	0.20
 <b>(2a)</b>	$2.7 \times 10^7$ <sup>b</sup>	DMF	50	2.64	0.22
			40	2.37	0.24
			25	2.05	0.27
			60	1.80	0.35
			50	1.47	0.41
			40	1.25	0.48
			100	1.43	0.52
			80	1.04	0.60
			60	0.68	0.89
			50	0.49	1.19
$M_n = 2400$	$D = 1.10$	EC	40	0.40	1.33
			25	0.37	1.47
			Hexane	3.06	0.19
			CH <sub>2</sub> Cl <sub>2</sub>	2.49	0.22
			THF	2.04	0.27
			Acetone-d <sub>6</sub>	3.24	0.18
			CD <sub>3</sub> CN	3.68	0.15
			100	0.994	0.010
			80	0.920	0.011
			60	0.836	0.012
		DMF	50	0.747	0.013
			40	0.692	0.016
			25	0.604	0.017
			60	0.56	0.022
			50	0.45	0.024
			40	0.36	0.026
			100	0.994	0.010
			80	0.920	0.011
			60	0.836	0.012
			50	0.747	0.013

<sup>a</sup>Molecular volume obtained as that contains within the 0.0010 electrons/bohr isosurface of electron density by theoretical calculation at the B3LYP/aug-cc-pVTZ level of theory.<sup>1</sup> <sup>b</sup>The molecule volume was calculated by hydrodynamic volume determined by dynamic light scattering.

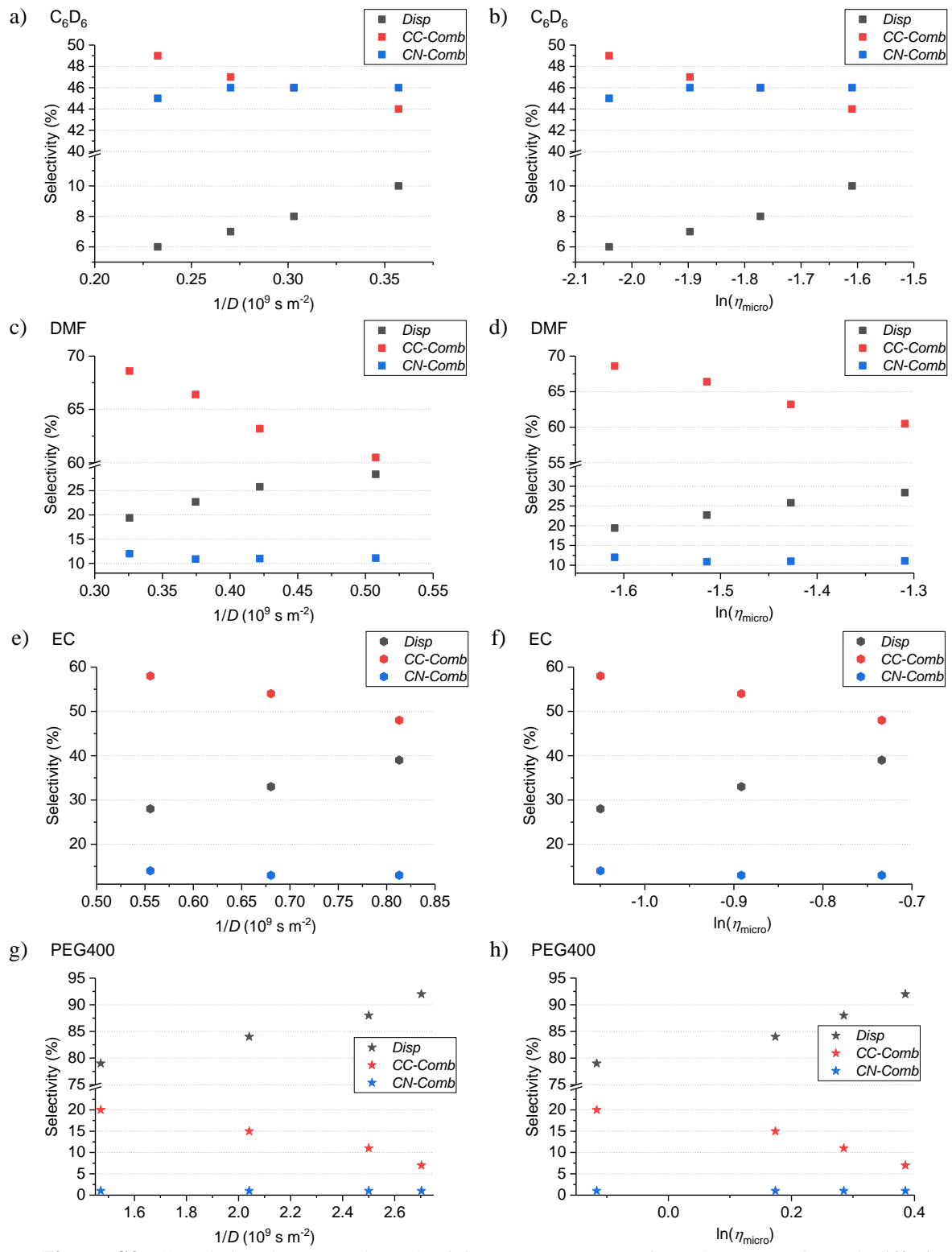


**Figure S3.** Correlation between the selectivity (*Disp*, *CC-Comb*, and *CN-Comb*) and diffusion constant or microviscosity in termination reaction of **1b** in (a, b)  $C_6D_6$ , (c, d) DMF, (e, f) EC, (g, h) PEG400 at various temperature (see Table S1).

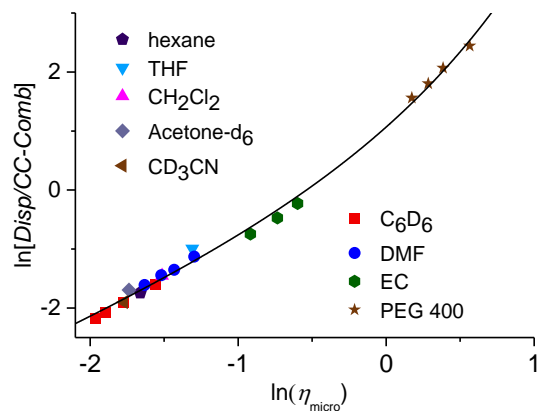


**Figure S4.** Correlation between *Disp/CC-Comb* selectivity and microviscosity in the termination reaction of **1b** in various solvents at different temperature (see Table S1).

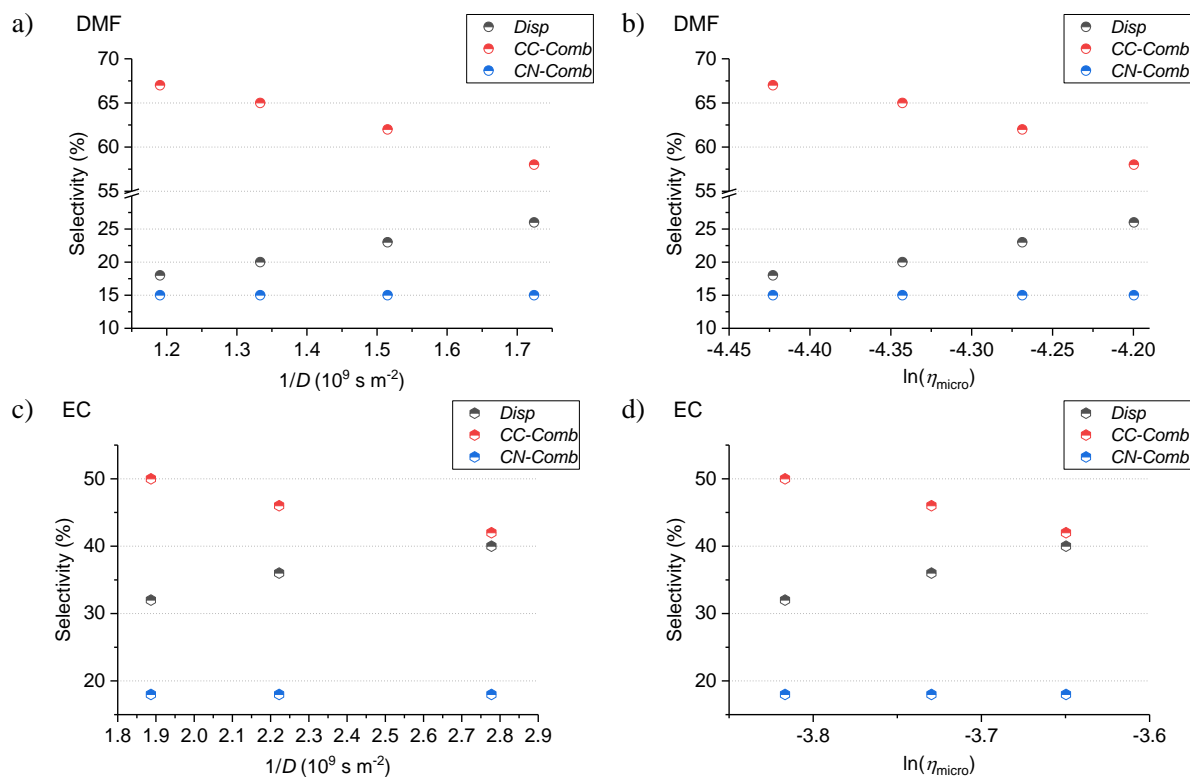


**Figure S5.** Correlation between the selectivity and diffusion constant or microviscosity in termination reaction of **1a** in (a, b) DMF, (c, d) EC at various temperature.

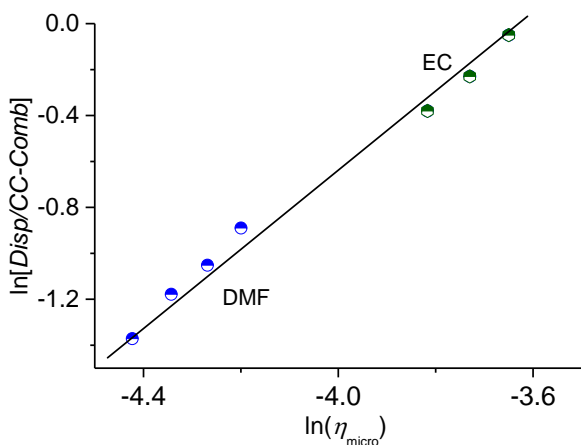


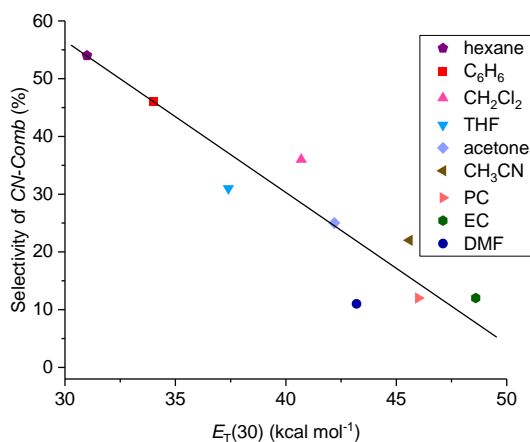
**Figure S6.** Correlation between the selectivity and microviscosity in termination reaction of **1a** in DMF and EC at various temperature.

#### 1-4. Analyses of the effect of the polarity parameters of solvents to the CN-Comb selectivity

**Table S3.** Solvent polarity parameters (25 °C) and the selectivity of *CN-Comb* in the termination reaction of **1b**.

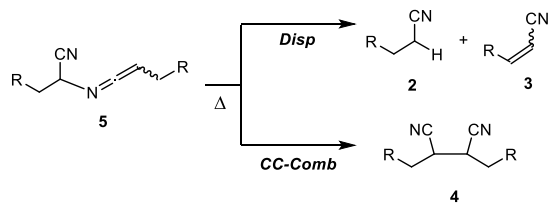
Solvent	Polarity index <sup>2</sup>	$E_T(30)$ (kcal mol <sup>-1</sup> ) <sup>3</sup>	Selectivity of <i>CN-Comb</i> (%)
Hexane	0.1	31.0	54
Benzene	2.1	34.3	46
CH <sub>2</sub> Cl <sub>2</sub>	3.1	40.7	36
THF	4.0	37.4	31
Acetone	5.1	42.2	25
CH <sub>3</sub> CN	5.8	45.6	22
Propylene carbonate <sup>a</sup>	6.1	46.0	12
Ethylene carbonate	- <sup>b</sup>	48.6 <sup>c</sup>	12
DMF	6.4	43.2	11

<sup>a</sup>Due to the unavailability of the polarity index of ethylene carbonate, that of propylene carbonate was used instead in this study. <sup>b</sup>The data was not available from literatures. <sup>c</sup>At 40 °C.



**Figure S7.** Correlation between the *CN-Comb* selectivity and the polarity parameter  $E_T(30)$  in the termination reaction of **1b** at 25 °C in various solvents

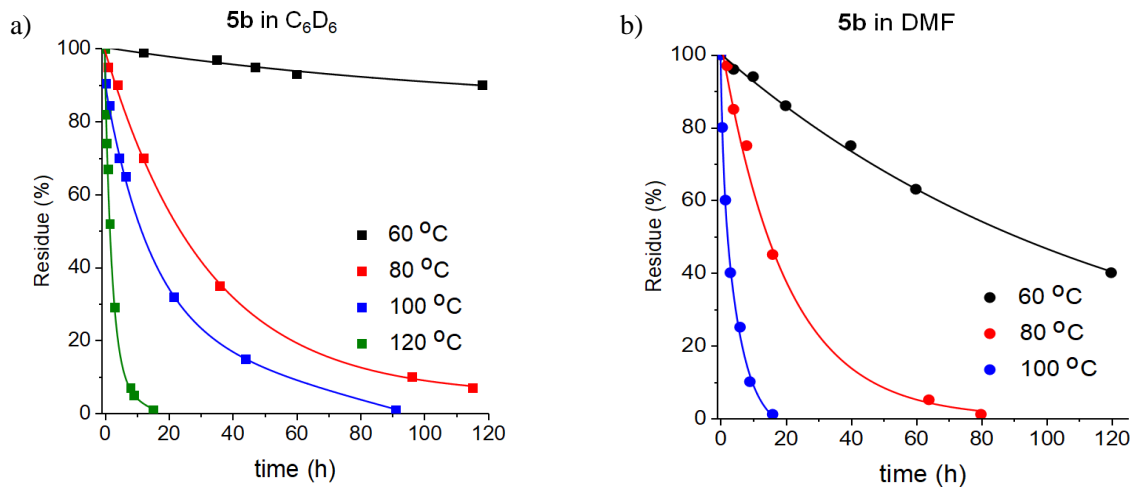
## 2. Thermal decomposition of 5



**Table S4. Thermal decomposition of 5 to giving 2, 3, and 4**

Run	Precursor	Solvent	Temp.	$\eta_{\text{bulk}}$	$D^a$ (°C)	$D^a$ (mPa·s)	$\times 10^{-9} \text{ m}^2 \text{ s}^{-1}$	Yield (%) <sup>b</sup>			$t_{1/2}^c$ CC- Comb (h <sup>-1</sup> )	$k^d$ (s <sup>-1</sup> )		
								2	3	4				
1	<b>5b</b>	C <sub>6</sub> D <sub>6</sub>	120	0.20	11.4	0.40	11.4	5	1	82	11	89	1.6	1.2 × 10 <sup>-4</sup>
2	<b>5b</b>	C <sub>6</sub> D <sub>6</sub>	100	0.25	9.50	0.46	9.50	6	2	80	12	88	12	1.7 × 10 <sup>-5</sup>
3	<b>5b</b>	C <sub>6</sub> D <sub>6</sub>	80	0.30	6.36	0.52	6.36	6	2	78	13	87	63	3.1 × 10 <sup>-6</sup>
4	<b>5b<sup>e</sup></b>	C <sub>6</sub> D <sub>6</sub>	60	0.36	4.30	0.60	4.30	1	<1	9	14	86	770	2.5 × 10 <sup>-7</sup>
5	<b>5b</b>	DMF	100	0.40	4.25	0.40	4.25	7	<1	76	12	88	2.5	8.2 × 10 <sup>-5</sup>
6	<b>5b</b>	DMF	80	0.46	3.56	0.46	3.56	6	<1	73	14	86	11	1.7 × 10 <sup>-5</sup>
7	<b>5b<sup>e</sup></b>	DMF	60	0.60	2.74	0.60	2.74	4	<1	51	16	84	89	2.2 × 10 <sup>-6</sup>
8	<b>5b</b>	PEG400	100	10	1.43	10	1.43	22	<1	44	50	50	4.6	4.2 × 10 <sup>-5</sup>
9	<b>5b</b>	PEG400	80	14	1.04	14	1.04	25	<1	41	55	45	29	6.4 × 10 <sup>-6</sup>
10	<b>5b<sup>e</sup></b>	PEG400	60	21	0.68	21	0.68	10	<1	13	60	40	330	1.4 × 10 <sup>-6</sup>
11	<b>5a</b>	DMF	100	0.82	0.994	0.82	0.994	- <sup>b</sup>	- <sup>b</sup>	- <sup>b</sup>	16	84	3.8	4.9 × 10 <sup>-5</sup>
12	<b>5a</b>	DMF	80	1.0	0.920	1.0	0.920	- <sup>b</sup>	- <sup>b</sup>	- <sup>b</sup>	18	82	19	8.8 × 10 <sup>-5</sup>
13	<b>5a</b>	DMF	60	1.2	0.836	1.2	0.836	- <sup>b</sup>	- <sup>b</sup>	- <sup>b</sup>	20	80	173	1.2 × 10 <sup>-6</sup>

<sup>a</sup>Diffusion constant. <sup>b</sup>Determined by <sup>1</sup>H NMR for model reactions for **5b** and SEC for **5a**. <sup>c</sup>Half-life time. <sup>d</sup>Reaction rate constant. <sup>e</sup>The conversion of **5b** in C<sub>6</sub>D<sub>6</sub>, DMF, PEG400 was 13%, 65% and 37% respectively.



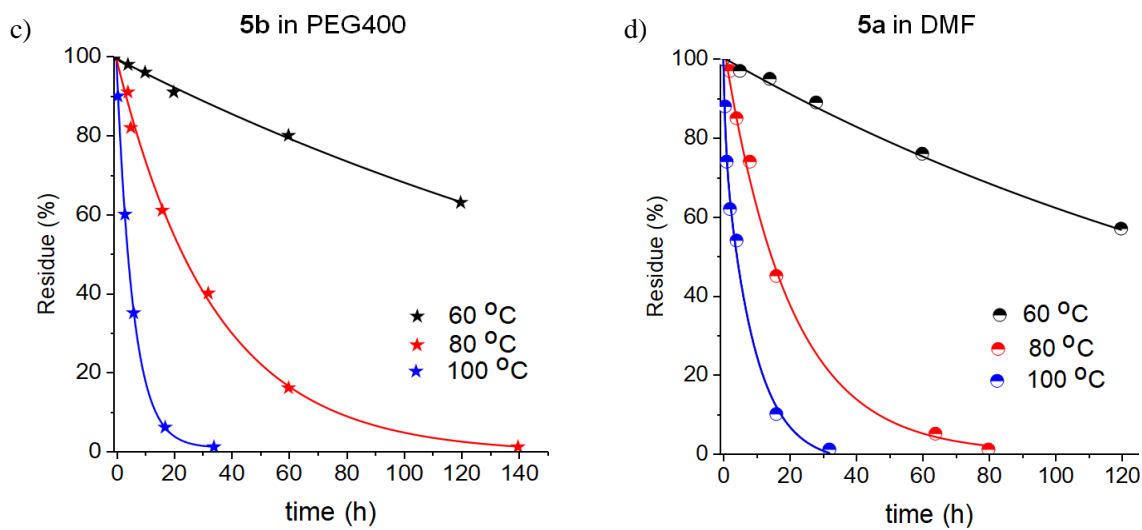


**Figure S8.** Kinetic plot of the thermal decomposition of **5**; (a) **5b** in  $\text{C}_6\text{D}_6$ , (b) **5b** in DMF, (c) **5b** in PEG400, (d) **5a** in DMF. The plots were fitted with first-order kinetic model.

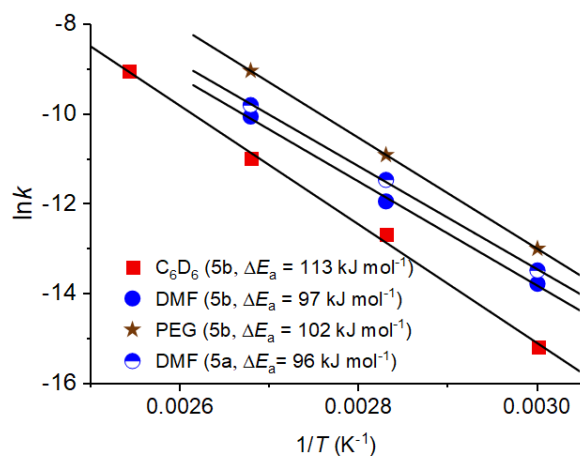


**Figure S9.** The Arrhenius plot for the thermal decomposition of **5** in various solvents and the activation energy ( $\Delta E_a$ ) determined from the plot.

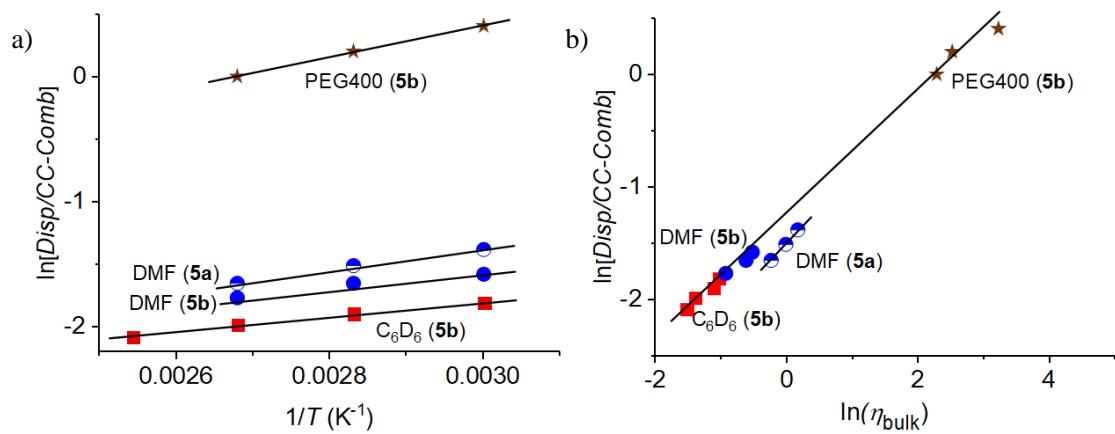


**Figure S10.** Correlation between the selectivity and (a) temperature or (b) bulk viscosity in termination reaction mechanism in each solvent at various temperature (see Table S4).

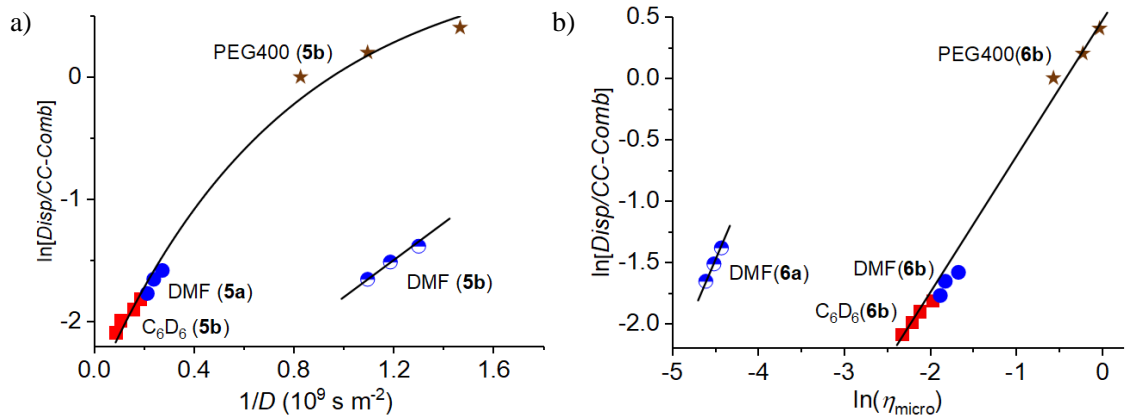


**Figure S11.** Correlation between the selectivity and (a) diffusion constant or (b) microviscosity in termination reaction mechanism in each solvent at various temperature (see Table S4).

### 3. NMR spectra

$^1\text{H}$  NMR

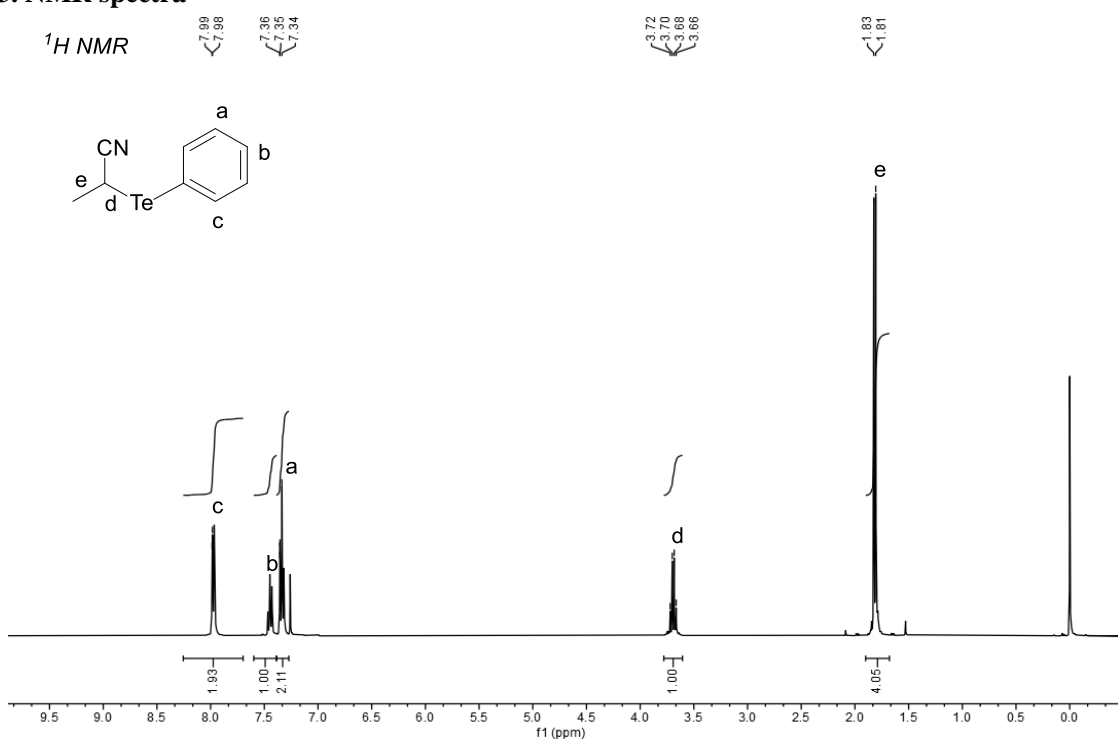


**Figure S12.**  $^1\text{H}$  NMR spectrum of 2-(phenyltellanyl)propanenitrile **6b** in  $\text{CDCl}_3$

$^{13}\text{C}$  NMR

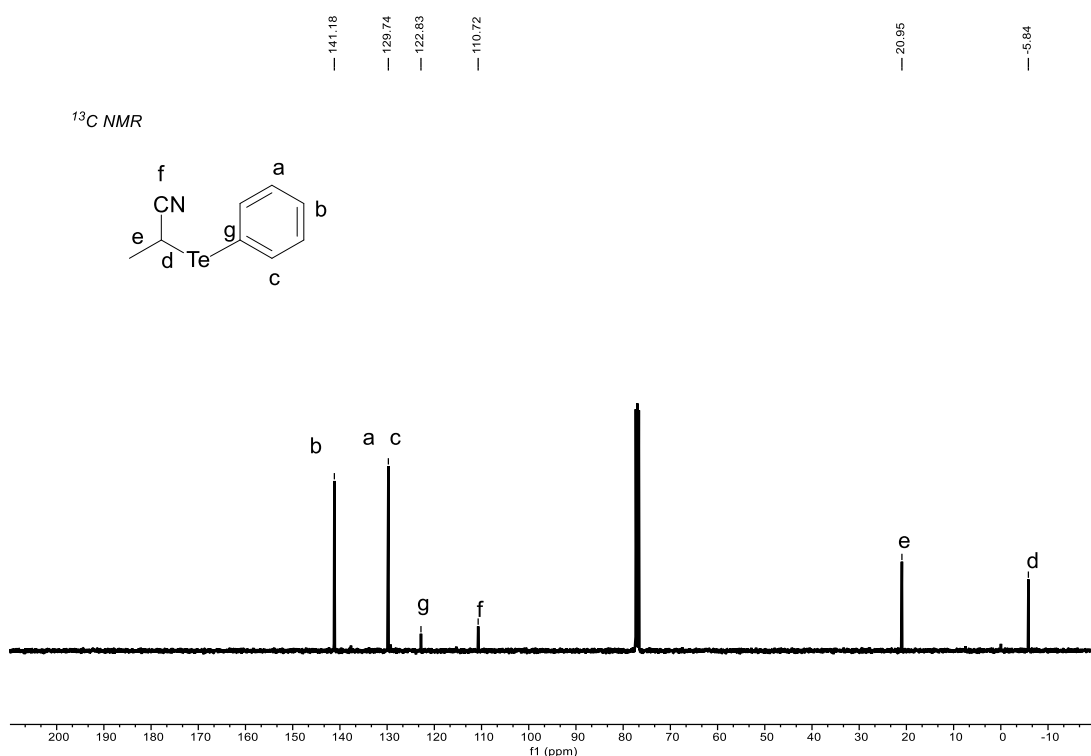


**Figure S13.**  $^{13}\text{C}$  NMR spectrum of 2-(phenyltellanyl)propanenitrile **6b** in  $\text{CDCl}_3$

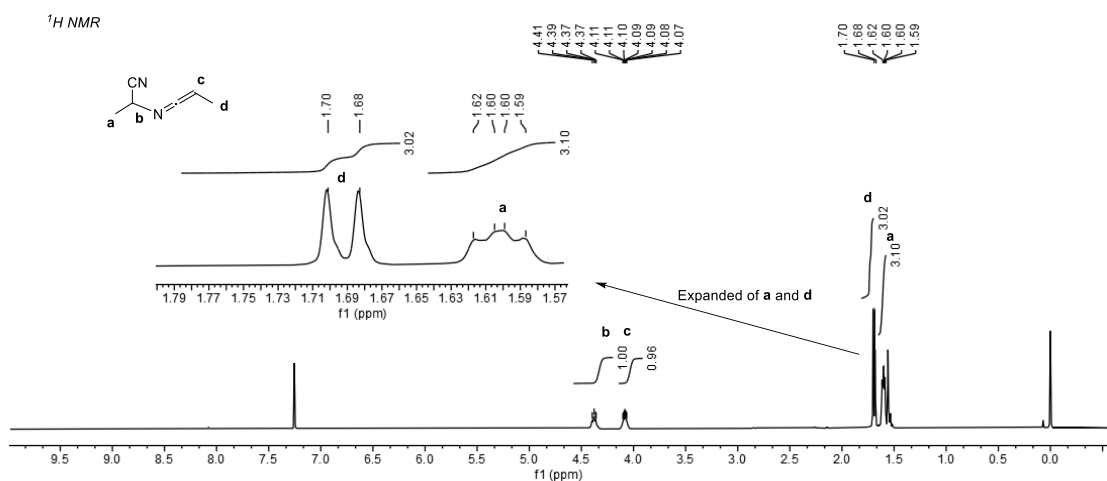


**Figure S14.** <sup>1</sup>H NMR spectrum of **5b** in CDCl<sub>3</sub>.

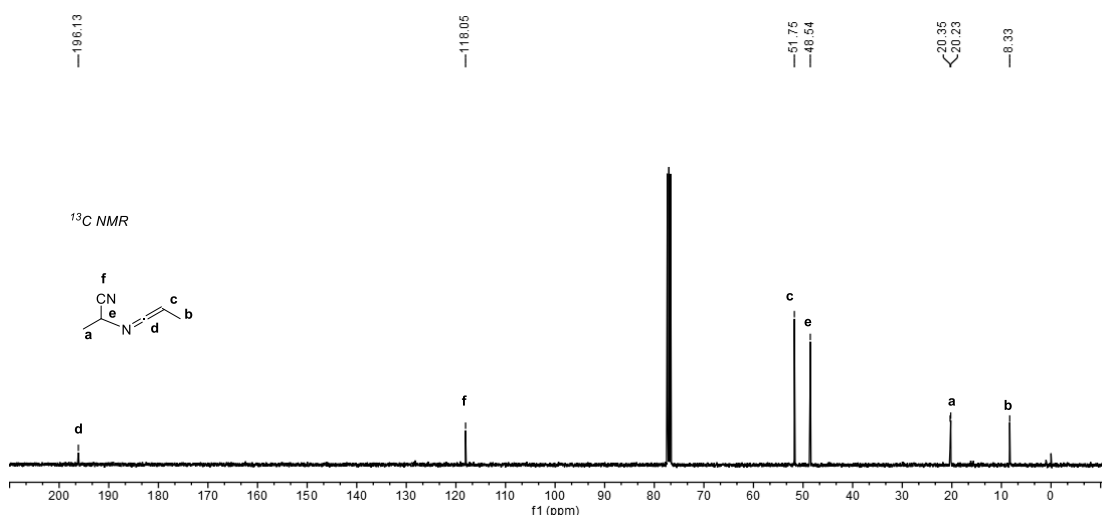


**Figure S15.** <sup>13</sup>C NMR spectrum of **5b** in CDCl<sub>3</sub>.

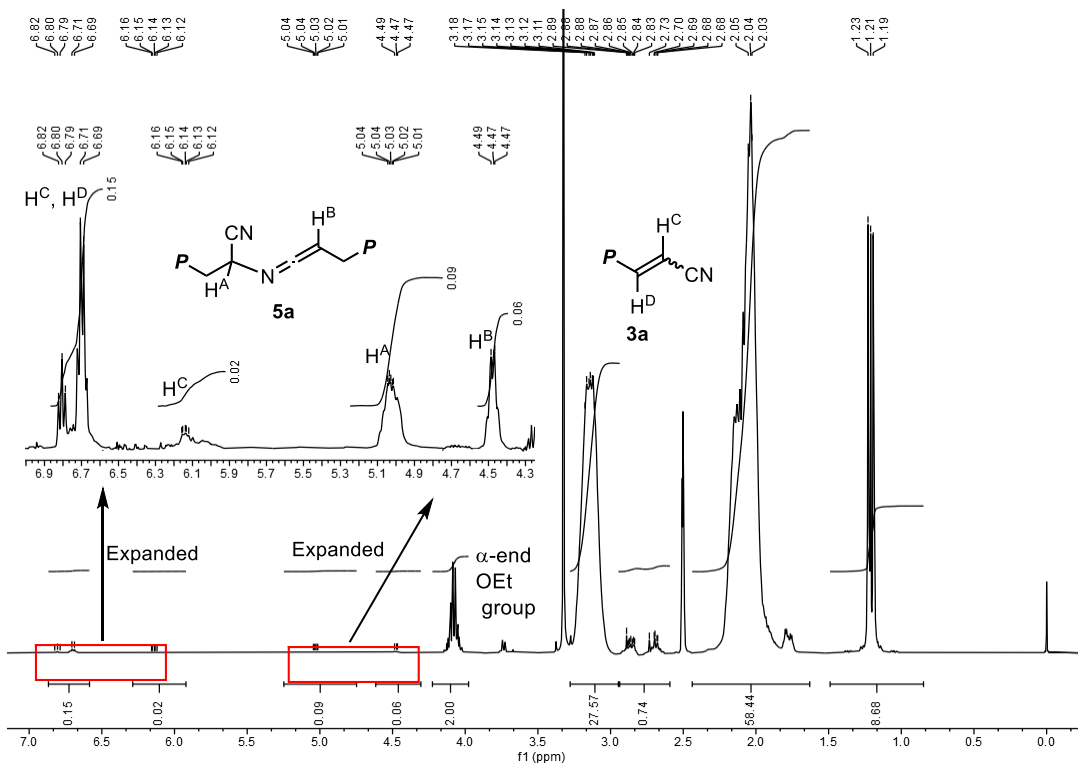


**Figure S16.**  $^1\text{H}$  NMR spectrum of the crude reaction mixture after photolysis of **6a** in DMF at  $60^\circ\text{C}$  (Table 1, run 21).

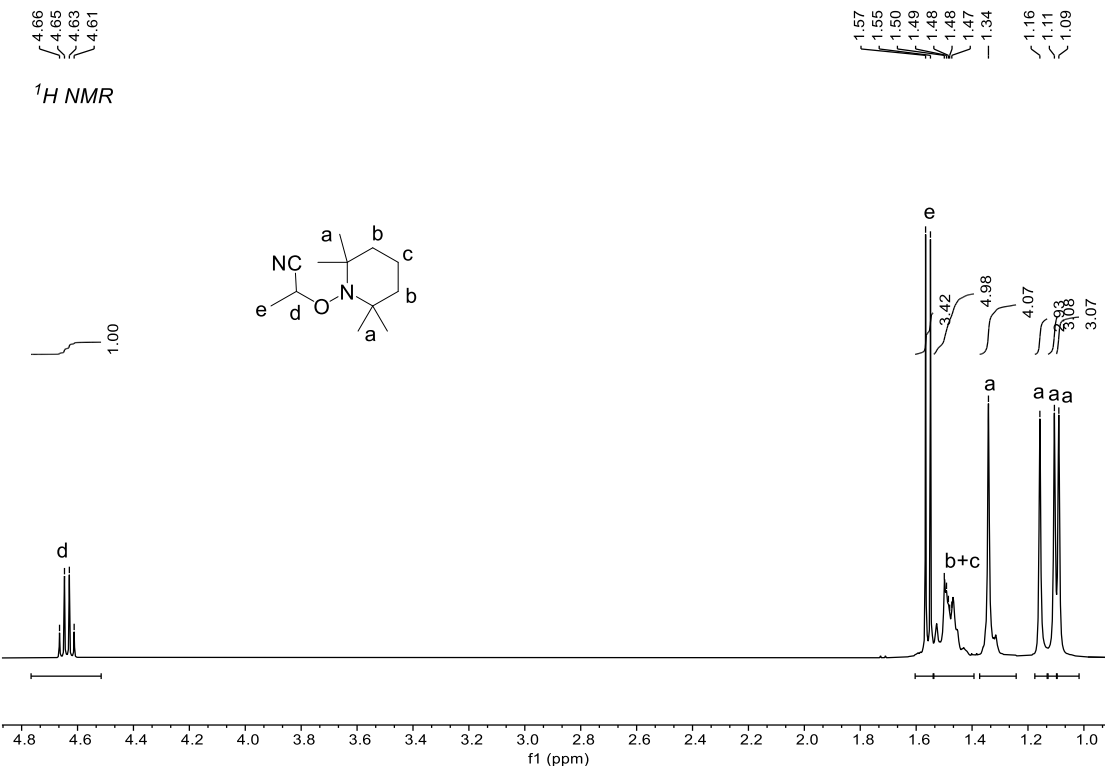


**Figure S17.**  $^1\text{H}$  NMR spectrum of 2-((2',2',6',6'-tetramethylpiperidin-1-yl)oxy)propanenitrile in  $\text{CDCl}_3$ .

#### 4. Cartesian coordinates<sup>1</sup>

a) molecular volume

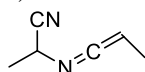
**1b**

C	1.635962	-0.33898	0
C	0.447659	0.570232	-2.2E-05
C	-0.86215	0.109612	-1E-06
N	-1.97122	-0.2854	0.000004
H	2.26553	-0.15147	-0.88022
H	2.265134	-0.15192	0.88061
H	1.343575	-1.39089	-0.00033
H	0.595489	1.646901	0.000049

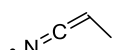
**2b**

C	1.561038	-0.448789	0.000055
C	0.484241	0.651645	-0.000204
C	-0.879641	0.110782	0.000229
N	-1.954035	-0.33095	-0.000023
H	2.554396	0.0087	0
H	1.472533	-1.08294	0.886051
H	1.472627	-1.083345	-0.885662
H	0.592468	1.296016	-0.880172
H	0.592389	1.296388	0.879467

b) Bond dissociation energy



C	-2.09283	-1.50932	0.121017
C	-1.13389	-0.32356	0.306479
N	-0.01496	-0.43517	-0.65748
C	1.149692	-0.45872	-0.25659
C	2.425462	-0.49495	0.061687
C	3.315858	0.723651	0.153366
C	-1.8281	0.958173	0.077441
N	-2.38609	1.964326	-0.07736
H	-1.56079	-2.44003	0.335046
H	-2.94362	-1.42118	0.801956
H	-2.45861	-1.54091	-0.9079
H	-0.76056	-0.30624	1.340561
H	2.855946	-1.47375	0.263259
H	2.767058	1.63851	-0.08323
H	3.73555	0.827822	1.160506
H	4.155209	0.640049	-0.54666



N	1.971406	-0.28527	-2.8E-05
C	0.862276	0.10947	0.000056
C	-0.4475	0.570045	-1.3E-05
C	-1.63626	-0.33893	-9E-06
H	-0.59601	1.646619	-3.7E-05
H	-1.34441	-1.39097	-0.00042
H	-2.26501	-0.15145	0.880772
H	-2.26548	-0.15086	-0.88032

	CN		
C	-1.63606	-0.33893	0.000008
C	-0.44762	0.570094	0.000012
C	0.862173	0.109523	-4E-06
N	1.971315	-0.28532	-1E-06
H	-2.26603	-0.15059	0.879779
H	-2.26485	-0.15223	-0.88096
H	-1.34389	-1.39086	0.001135
H	-0.59539	1.64678	-4.4E-05

## 5. References

1. All computational calculations were performed using Gaussian 16 suite. The geometry optimizations and frequency calculations were carried out at the B3LYP/6-31+G(d,p) level of theory. The molecular volume was defined as that contained within the 0.0010 electrons/bohr<sup>3</sup> isosurface of electron density, and calculated at the B3LYP/aug-cc-pVTZ level of theory.
2. Snyder, L. R. *J. Chromatogr. Sci.* **1978**, *16*, 223-234.
3. Reichardt, C. *Chem. Rev.* **1994**, *94*, 2319-2358.